Density of constitutional and thermal point defects in $L1_2$ Al_3Sc

C. Woodward*
Air Force Research Laboratory, Materials and Manufacturing Directorate, Wright Patterson Air Force Base, Dayton, Ohio 45433-7817

M. Asta
Department of Materials Science and Engineering, Northwestern University, Evanston, Illinois 60208

G. Kresse and J. Hafner
The Institut für Materialphysik of the Universität Wien, Wien, Austria
(Received 18 August 2000; published 26 January 2001)

The energy of constitutional and thermal point defects in $L1_2$ Al_3Sc are calculated within a first principles, local density functional theory framework. Relaxed structures and energies for vacancies and antisites are calculated using a plane-wave pseudopotential method. The resulting energies are used within a dilute-solution thermodynamic formalism to estimate the equilibrium point defect densities as functions of temperature and alloy composition. The first-principles-based thermodynamic calculations predict that Al_3Sc forms antisite constitutional defects for both Al- and Sc-rich alloys. Also, the density of thermal vacancies is found to be very sensitive to the underlying stoichiometry. At 1000 K the Sc-sublattice vacancy concentration increases by ten orders of magnitude as the alloy goes from Sc to Al rich. At this temperature, the density of Sc-sublattice vacancies is predicted to be comparable to the concentration of Al antisite defects for Al-rich alloys.

DOI: 10.1103/PhysRevB.63.094103 PACS number(s): 61.72.Ji, 61.72.Ss, 62.20.Dc, 81.05.Zx

I. INTRODUCTION

The mechanical properties and phase stability of the Al_3Sc intermetallic compound have been topics of substantial experimental and theoretical research over the past decade. This compound is one of only seven binary trialuminide intermetallics forming in the cubic $L1_2$ structure under equilibrium conditions. As a consequence, Al_3Sc represents a model system for studying the deformation modes and intrinsic brittleness of cubic trialuminides, and detailed experimental investigations of plastic deformation and fracture in this compound have been undertaken,[1–4] combined with first-principles calculations of elastic and defect properties.[5] The Al_3Sc phase plays a critical role as a precipitate strengthener in heat-treated Al(Sc) alloys. Sc is known to be the most potent strengthener of Al alloys (per atomic percent)[6,7] due to the homogeneous formation of the Al_3Sc phase as coherent precipitates in supersaturated Al(Sc) alloys aged at between 300 and 350 °C. The thermodynamic factors underlying precipitation of Al_3Sc have been the topic of two recent first-principles theoretical investigations.[8,9] The Al-rich portion of the Al-Sc phase diagram and free energies of coherent Al/Al_3Sc interfacial free energies were calculated by Asta, Foiles, and Quong[8] using a cluster-expansion approach.[10,11] Recently, the results of this study were combined with first-principles calculations of ionic vibrational entropies leading to highly improved accuracy for calculated solid-solubility limits of Sc in Al.[9]

As a basis for further improving the high-temperature properties of Al-Sc alloys, the effects of ternary additions upon the stability and mechanical properties of Al_3Sc have begun to be investigated experimentally. Very recently, Harada and Dunand[12] have investigated the effects of ternary additions upon high-temperature mechanical properties in ternary $Al_3(Sc_{0.74}X_{0.26})$ alloys, with $X=$Ti, Y, Zr, and Hf. These authors measured creep rates that decreased by one to two orders of magnitude as a result of ternary alloying. Creep processes, produced by strains below the critical shear stress, are typically rate limited by diffusion. As a preliminary step toward investigating the diffusive component of creep resistance in ternary alloys, we present here the results of a first-principles study of point defects in binary Al_3Sc. In this study the structure and energies of vacancies and antisite point defects are calculated using a plane-wave pseudopotential method in the local-density approximation. These energies are used in a grand-canonical, dilute-solution model (DSM) thermodynamic formalism to predict equilibrium defect concentrations as a function of alloy composition and temperature. The DSM formalism has been used in a number of computational studies of equilibrium point-defect concentrations in intermetallic compounds, with point-defect energies calculated either from classical interatomic potentials or first-principles electronic-structure methods.[13–27] Applications of the first-principles DSM in ternary TiAl-X ($X=$Si, Nb, Mo, Ta, and W) alloys have been very successful in estimating the site selection of ternary additions, defect formation energies, and trends in thermal-defect concentrations as a function of alloy chemistry and temperature.[20]

II. METHOD

The thermodynamic formalism underlying the DSM has been reviewed in detail recently by Mishin and Herzig,[27] and we present here an alternative formulation of the model based upon the statistical-mechanical formalism of low-temperature expansions (LTE).[28] In the limit of dilute defect concentrations, the expressions for equilibrium defect densities presented below can be shown to be equivalent to those derived using a Bragg-Williams model for the configurational entropy.[20,27] The LTE formulation is presented here as

a more general formalism that can be used as a basis for incorporating the effects of defect interactions for nondilute concentrations.

Consider a crystalline alloy compound with N lattice sites, and define N_i to be the number of sites occupied by chemical species i. For what follows it is useful to introduce a site-occupation variable $c_i(\mathbf{p})$ that is 1 if lattice site $\mathbf{p}$ is occupied by species i, and 0 otherwise. In the thermodynamic model formulated below we consider vacancies explicitly, and a vacant lattice site is signified by $c_i(\mathbf{p})=0$, for all chemical species i. The number of atoms of species i is given by the sum $N_i=\Sigma_{\mathbf{p}}c_i(\mathbf{p})$.

We are interested in calculating the equilibrium number density of vacancies and antisite defects on each sublattice of an ordered intermetallic compound as a function of alloy composition and temperature. For this purpose it is convenient to work in a grand-canonical formalism, employing a thermodynamic potential $\Omega(\{\mu_i\},T,V,N)$, where V and T denote the crystal volume and the temperature, respectively. The Ω potential is related to the more familiar Helmholtz free energy (F) through the Legendre transformation: $\Omega=F-\Sigma_i\mu_iN_i$, where μ_i are the chemical potentials of species i.

The Ω potential can be written formally as $\Omega=-k_BT\ln Z$, where k_B is Boltzmann's constant, in terms of a partition function Z defined as follows (neglecting nonconfigurational contributions to the alloy free energy):

$$Z=\sum_{\sigma}\ \exp\left[-\left(E^{\sigma}-\sum_{i}\ \mu_iN_i^{\sigma}\right)\Big/\ k_BT\right], \tag{1}$$

where the sum is over all possible arrangements (σ) of atoms over the N lattice sites. In Eq. (1), E^{σ} and N_i^{σ} denote the energy and number of sites occupied by species i, respectively, for configuration σ. By factoring out the ground-state energy from Eq. (1), and using a Taylor's series expansion for the logarithm, the first-order LTE expression for the Ω potential can be formulated as follows:

$$\begin{aligned}\Omega=&\left[E^0-\sum_{i}\ \mu_i\sum_{\mathbf{p}}\ c_i^0(\mathbf{p})\right]\\&-k_BT\sum_{\mathbf{p}}\ \sum_{\epsilon}\ \exp\Bigg\{-\Bigg[\delta E^{\epsilon}(\mathbf{p})\\&-\sum_{i}\ \mu_i\delta c_i^{\epsilon}(\mathbf{p})\Bigg]\Big/\ k_BT\Bigg\}.\end{aligned} \tag{2}$$

In Eq. (2), E^0 and $c_i^0(\mathbf{p})$ denote the energy and composition of species i at site $\mathbf{p}$, respectively, in the ground-state configuration (corresponding to binary, stoichiometric Al_3Sc in the present study). The second term on the right-hand side of Eq. (2) represents a sum over first-order ''spin-flip excitations.'' The excitations correspond to the different possible changes (ϵ) of chemical identity at a given lattice site $\mathbf{p}$. In particular, if site $\mathbf{p}$ is on an Al sublattice of the Al_3Sc compound, the excitations ϵ involve Al→Sc and Al→vacancy. In discussing the different possible excitations, we adopt the conventional notation for the point defects where V_{Al} and Sc_{Al} denote a vacancy and antisite Sc atom on the Al sublattice, respectively, and similarly for V_{Sc} and Al_{Sc}. The variables $\delta E^{\epsilon}(\mathbf{p})$ and $\delta c_i^{\epsilon}(\mathbf{p})$ in Eq. (2) denote the change in energy and site-composition, respectively, associated with excitation ϵ at site $\mathbf{p}$. In what follows we will refer to $\delta E^{\epsilon}(\mathbf{p})$ as an ''excitation energy'' whereas the total quantity in the exponential in Eq. (2), $[\delta E^{\epsilon}(\mathbf{p})-\Sigma_i\mu_i\delta c_i^{\epsilon}(\mathbf{p})]$, is the defect formation energy.

The average concentration of species i on lattice site $\mathbf{p}$, $\langle c_i(\mathbf{p})\rangle$, can be derived from Eq. (2) using the thermodynamic relationship $\langle c_i(\mathbf{p})\rangle=-\partial\Omega/\partial\mu_i(\mathbf{p})$, as follows:

$$\begin{aligned}\langle c_i(\mathbf{p})\rangle=&c_i^0(\mathbf{p})+\sum_{\epsilon}\ \delta c_i^{\epsilon}(\mathbf{p})\\&\times\exp\left\{-\left[\delta E^{\epsilon}(\mathbf{p})-\sum_{j}\ \mu_j\delta c_j^{\epsilon}(\mathbf{p})\right]\Big/\ k_BT\right\}.\end{aligned} \tag{3}$$

Equation (3) expresses the defect concentrations in terms of the chemical potentials. For an alloy with n chemical species (excluding vacancies), the values of the chemical potentials at a given temperature are fixed by specifying the $n-1$ relative compositions N_i/N_j. Also there is the additional requirement, arising from conditions for point defect equilibrium, that Ω vanishes at zero pressure.[29] From these n constraints the chemical potentials at a given alloy composition and temperature are determined, and the sublattice antisite and vacancy concentrations can be calculated from Eq. (3).

It is worth mentioning that the first-order LTE formalism leading to the expressions given in Eqs. (2) and (3) can be generalized by including higher-order terms in the expansion of the Ω potential. The first-order expressions used in this work are expected to be accurate for dilute defect concentrations, i.e., less than roughly 1%. For more concentrated compositions, higher-order terms in the expansion of the thermodynamic potential Ω are expected to give rise to appreciable changes in the values of the chemical potentials and defect densities, reflecting the effects of defect-defect interactions. We emphasize that the LTE formalism can be generalized straightforwardly beyond the first-order framework outlined above. A second-order LTE can be formulated including excitations involving pairs of lattice sites. For example, in the work of Asta *et al.*[8] a second-order LTE formalism was used to calculate phase boundaries and interfacial thermodynamic properties of Al-Sc alloys. In this previous work the pair and point excitation energies were derived from a first-principles-based cluster expansion of the configurational energy for fcc-based Al-Sc alloys.

III. COMPUTATIONAL DETAILS

The point defect ''excitation'' energies in Al_3Sc are calculated using the Vienna *ab initio* simulation package (VASP).[30–32] Ultrasoft pseudopotentials are used to approximate the electron-ion interactions with a plane-wave cutoff energy of 150.69 eV.[33,34] Bands near the Fermi surface are partially occupied using finite temperature broadening as proposed by Methfessel and Paxton.[35] In order to test the

TABLE I. Calculated equilibrium lattice parameters and elastic molduli (Mbar) for Al_3Sc. The results of previous electronic structure studies are also included.

Method	a (Å)	K	C_{11}	C_{12}	C_{44}
VASP	4.038	0.92	1.91	0.43	0.82
FLAPW [a]	4.04	0.92	1.89	0.43	0.66
ASA-LMTO [b]	4.055	0.93			
NCPP [c]	4.008	0.96			
Experimental [d]	4.101 [e]	0.92	1.83	0.46	0.68

[a]Reference 5.
[b]Atomic sphere approximation–linear muffin tin orbital, Ref. 38.
[c]Norm-conserving pseudo-potential, Ref. 9.
[d]Reference 39.
[e]Reference 40.

reliability of the pseudopotentials, structural parameters were calculated for the Al_3Sc, $L1_2$ cubic unit cell. The lattice constant and bulk modulus are determined by fitting the total energy as a function of hydrostatic strain to Murnaghans equation of state.[36] Similarly the elastic constants are determined by applying symmetry-restricted strains to the lattice and fitting the energy dependence to second- and fourth-order polynomials.[20] The predicted lattice constants, bulk modulus and elastic constants are shown in Table I. The lattice parameter and bulk modulus are in good agreement with previous full potential–linear augmented plane wave (FP-FLAPW) calculations and available experimental data (Table I).

IV. RESULTS

A. Electronic structure and defect energies

Al_3Sc is an ordered $L1_2$, fcc derivative structure, consisting of a conventional fcc Al unit cell with the atoms at the corners of the cell replaced by Sc atoms. Figures 1(a) and 1(b) show the charge density for mixed and all Al (010) planes, respectively. The mixed planes illustrate the Sc d electrons polarized in the $\langle 110 \rangle$ direction, towards a nearest neighbor Al atom. This is in good agreement with previous FLAPW calculations.[5] Also, in the all-Al plane, Al p electrons are weakly polarized along $\langle 110 \rangle$-type directions between nearest-neighbor Al atoms. Directional bonding of this nature is often observed in the transition-metal–aluminum intermetallics. Details of the bonding have also been used to rationalize the trends in planar fault[41] and surface energies.[5]

The structure and energy of the point defects were calculated in two steps. First the point defects were introduced into an otherwise perfect lattice represented by a 64-atom supercell. The self-consistent electronic structure was calculated for this configuration using a plane-wave cutoff of 150.69 eV. These calculations employed 63 Monkhorst-Pack special k points and a broadening parameter of 0.10 eV.[37] Next, the positions of the first- and second-nearest-neighbor atoms were optimized using a conjugate gradient procedure until the vector components of the force on any atom was less than 0.01 eV/Å. This converges the total energy to better than 0.01 eV. The change in energy produced by forming

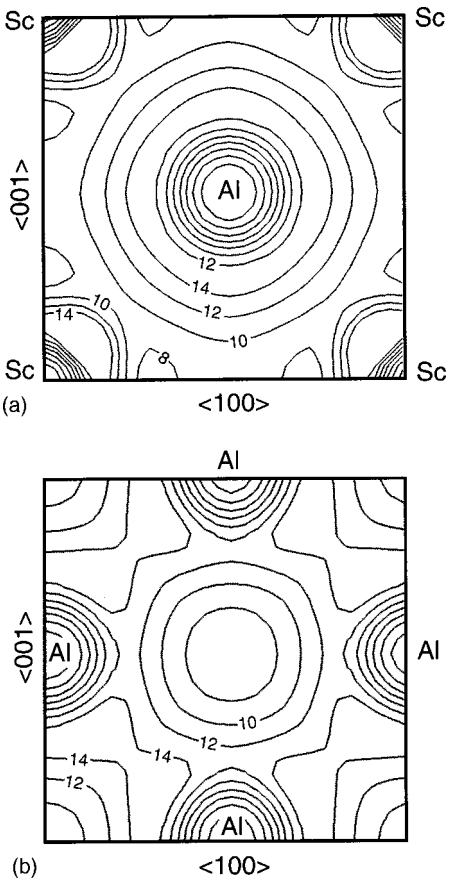

FIG. 1. Charge density contour plots of the (a) (100) mixed plane and the (b) (100) all Al plane. Charge density contours are labeled in units of 10^{-3} electron/a.u.^{3}

these defects relative to the bulk is sometimes referred to as raw defect energy.[25] The numerical values for the raw defect energies that we identify as excitation energies $[\delta E^{\epsilon}(\mathbf{p})]$ are shown in Table II. Expressions for the defect formation energies will be developed in the discussion section. Optimizing the positions of the first- and second-nearest-neighbor atoms around the defect can reduce the defect energies by as much as 0.2 eV. Changes in defect energies of this magnitude significantly change the predicted density of thermal defects. Here we assume that the defects prefer the lattice site, no attempt was made to break the symmetry of the defect centers. For some of the defects additional strain energy may be realized by relaxing the third-nearest-neighbor atoms. However, in most cases considered here, the lattice

TABLE II. Calculated excitation energies, δE (eV) for vacancy and antisite point defects in Al_3Sc.

Defect	Point defects: Unrelaxed	Point defects: $\bar{R}_{\text{ions}}$ optimized
V_{Al}	5.949	5.793
V_{Sc}	9.448	9.244
Sc_{Al}	−1.463	−1.569
Al_{Sc}	5.281	5.200

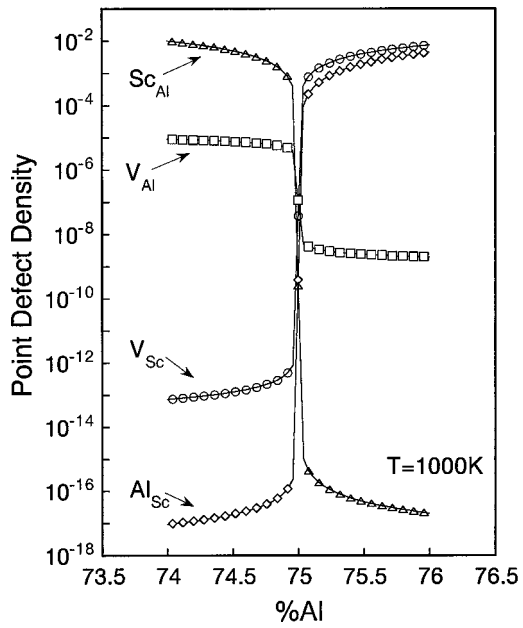

FIG. 2. Predicted point defect densities at 1000 K as a function of stoichiometry.

misfit is small and the strain energy from the displacement of atoms in more distant neighbor shells was estimated to be less than 0.01 eV. The calculated displacements of the first- and second-nearest-neighbor atoms are typically less than 1% of the lattice constants.

B. Defect densities

To calculate defect concentrations as functions of temperature and alloy composition the defect excitation energies given in Table II have been used in the DSM as described in Sec. II. The predicted defect concentrations as a function of alloy composition $N_{\mathrm{Al}}/(N_{\mathrm{Al}}+N_{\mathrm{Sc}})$ at a temperature of 1000 K are shown in Fig. 2. Al_3Sc is stable over a narrow range of composition, so we present results within 1% of stoichiometry. As the composition changes from Sc to Al rich, the chemical potentials (μ_{Al} and μ_{Sc}) change in order to accommodate the formation of constitutional defects. We find a large concentration of antisites on either side of stoichiometry. Also, the density of Sc vacancies (V_{Sc}) is quite large, larger in fact than the concentration of Al antisites ($\mathrm{Al_{Sc}}$), for Al-rich materials at 1000 K. Reducing the temperature leads to a rapid decrease in the equilibrium V_{Sc} concentration for Al-rich alloys, with the number density of Sc vacancies being an order of magnitude smaller than the concentration of $\mathrm{Al_{Sc}}$ antisites at 200 K. Therefore, antisites are by definition constitutional defects while the V_{Sc} population arises by thermal excitations.

V. DISCUSSION

The numerical results presented in Fig. 2 can be understood qualitatively based upon an analysis of the relative defect excitation energies listed in Table II. First we derive which point defects are produced by compositional disorder when the alloy composition deviates from stoichiometry.

TABLE III. Differences in formation energies (eV) for the point defect complexes that lead to equivalent changes in alloy composition, as defined in Eqs. (5) and (7). Expressions are evaluated using the calculated defect energies in Table II and the energy of enthalpy per atom in the bulk material [e.g., $E_{\mathrm{ref}}=E^0/N=(3\mu_A+\mu_B)/4$].

$\Delta E(V_{\mathrm{Sc}},\mathrm{Al_{Sc}})$	$\Delta E(V_{\mathrm{Al}},\mathrm{Sc_{Al}})$
$4\delta E^V(\mathrm{Sc})-3\delta E^{\mathrm{Al}}(\mathrm{Sc})+4E_{\mathrm{ref}}$	$4\delta E^V(\mathrm{Al})-\delta E^{\mathrm{Sc}}(\mathrm{Al})+4E_{\mathrm{ref}}$
0.172	3.537

Off-stoichiometric alloy compositions can be accomodated through the different point defects listed in Table II. An Al composition greater than 0.75 can be realized either through $\mathrm{Al_{Sc}}$ antisites or V_{Sc} vacancies. The former gives rise to a ratio of the Al to Sc compositions of $(N_{\mathrm{Al}}+m)/(N_{\mathrm{Sc}}-m)$, where m is the number of antisites. Similarly, n Sc vacancies lead to a composition ratio of $N_{\mathrm{Al}}/(N_{\mathrm{Sc}}-n)$. Starting from a stoichiometric alloy, $N_{\mathrm{Al}}/N_{\mathrm{Sc}}=3$, and considering only small changes in alloy composition, it can be shown that $m=3$ antisites and $n=4$ Sc vacancies give rise to equivalent increases in the Al composition. The probability of forming a complex of four Al antisites is given by the fourth power of the probability of forming a single $\mathrm{Al_{Sc}}$ defect, assuming dilute concentrations. Similarly the probability of a triple Sc-vacancy complex is given as the third power of the single-defect concentration. From Eq. (3) we can write the relative probability of forming these two defect complexes as

$$\frac{\langle c_V(\mathrm{Sc})\rangle^4}{\langle c_{\mathrm{Al}}(\mathrm{Sc})\rangle^3}=\exp[-\Delta E(V_{\mathrm{Sc}},\mathrm{Al_{Sc}})/k_BT], \tag{4}$$

where the difference in defect formation energies, $\Delta E(V_{\mathrm{Sc}},\mathrm{Al_{Sc}})$ is given as

$$\Delta E(V_{\mathrm{Sc}},\mathrm{Al_{Sc}})=4\delta E^V(\mathrm{Sc})-3\delta E^{\mathrm{Al}}(\mathrm{Sc})+(3\mu_{\mathrm{Al}}+\mu_{\mathrm{Sc}}). \tag{5}$$

It can be argued in a similar way that one Sc antisite defect, $\mathrm{Sc_{Al}}$, gives rise to the same decrease in Al composition as four Al vacancies, V_{Al}. The relative concentrations of the relevant defect complexes in this case can be written as

$$\frac{\langle c_V(\mathrm{Al})\rangle^4}{\langle c_{\mathrm{Sc}}(\mathrm{Al})\rangle}=\exp[-\Delta E(V_{\mathrm{Al}},\mathrm{Sc_{Al}})/k_BT], \tag{6}$$

with the difference in defect formation energies given by

$$\Delta E(V_{\mathrm{Al}},\mathrm{Sc_{Al}})=4\delta E^V(\mathrm{Al})-\delta E^{\mathrm{Sc}}(\mathrm{Al})+(3\mu_{\mathrm{Al}}+\mu_{\mathrm{Sc}}). \tag{7}$$

At low temperatures, very close to stoichiometry, the combination of chemical potentials $3\mu_{\mathrm{Al}}+\mu_{\mathrm{Sc}}$ entering Eqs. (5) and (7) is approximately equal to four times the energy (per atom) of the reference Al_3Sc crystal. From this estimate for the chemical potentials, and the values of the excitation energies given in Table II, the numbers for $\Delta E(V_{\mathrm{Sc}},\mathrm{Al_{Sc}})$ and $\Delta E(V_{\mathrm{Al}},\mathrm{Sc_{Al}})$ listed in Table III are derived. Note that both quantities are positive, with $\Delta E(V_{\mathrm{Al}},\mathrm{Sc_{Al}})$ much larger in magnitude than $\Delta E(V_{\mathrm{Sc}},\mathrm{Al_{Sc}})$. For very low temperatures, Eqs. (4) and (6) predict vanishingly small vacancy concen-

TABLE IV. Expressions and numerical values for the μ_{Al} and μ_{Sc} (in eV) for stoichiometric Al_3Sc and for small deviations from stoichiometry. The numerical values are based on the defect energies presented in Table II.

	Composition		
	Al rich	Stoichiometric	Sc rich
μ_{Al}	$E_{ref}+\delta E^{Al}(Sc)/4$	$E_{ref}+(\delta E^{Al}(Sc)-\delta E^{Sc}(Al))/8$	$E_{ref}-\delta E^{Sc}(Al)/4$
	-4.001	-4.455	-4.909
μ_{Sc}	$E_{ref}-3\,\delta E^{Al}(Sc)/4$	$E_{ref}+3(\delta E^{Sc}(Al)-\delta E^{Al}(Sc))/8$	$E_{ref}+3\,\delta E^{Sc}(Al)/4$
	-9.201	-7.839	-6.477

trations, relative to the equilibrium densities of antisites, consistent with the numerical results discussed at the beginning of the section. Therefore this alloy accomodates deviations from stochiometry by forming antisite defects.

Equations (4) and (6), along with the defect formation energy differences given in Table III, can also be used to understand why the thermal Sc vacancy concentration is so much larger, for Al-rich compositions, than the Al-vacancy concentration for Sc-rich compositions. From Eq. (4) we see that, for fixed chemical potentials, the Sc-vacancy concentration increases with temperature, with $\langle c_V(Sc)\rangle$ approaching $\langle c_{Al}(Sc)\rangle^{3/4}$ in the limit of high T. In light of the relatively small value of $\Delta E(V_{Sc},Al_{Sc})$ given in Table III, it is possible to understand qualitatively how the thermal Sc-vacancy concentration can become larger than the Al antisite concentration at high temperatures. For Sc-rich alloys the Al-vacancy concentration remains relatively small. The much larger value $\Delta E(V_{Al},Sc_{Al})$ in Table III implies that high vacancy concentrations can only be realized at temperatures very much higher than 1000 K.

For estimating starting values for the numerical DSM calculations, and to gain further insight into the numerical results presented in Fig. 2, it is useful to use Eqs. (2) and (3) to derive approximate values of the chemical potentials for off-stoichiometric alloys at low temperatures. Specifically, once the dominant constitutional defect has been identified, as above, Eq. (3) can be approximated keeping only the term corresponding to this lowest-energy excitation. The resulting approximate equation can be used to derive a relation between the chemical potentials and the constitutional defect concentration. For example, for Al-rich compositions, Eq. (3) gives $\mu_{Al}-\mu_{Sc}\approx\delta E^{Al}(Sc)+k_BT\ln\langle c_{Al}(Sc)\rangle$. For low temperatures such that k_BT is much smaller in magnitude than $\delta E^{Al}(Sc)$ this relation takes a limiting form of $\mu_{Al}-\mu_{Sc}\approx\delta E^{Al}(Sc)$. Furthermore, a similar argument based upon Eq. (2) can be used to derive the approximate relationship $3\mu_{Al}+\mu_{Sc}\approx 4E^0$. From these two relations the estimated chemical potential values for Al-rich compositions given in Table IV are obtained. The values for Sc-rich compositions are derived in an analogous manner. For each thermal defect the chemical potential estimates given in Table IV, and the excitation energies listed in Table II, are used to derive the values of the defect formation energies listed in Table V. From this table we see that the formation energy for a Sc vacancy in Al-rich alloys is very low, consistent with the high thermal concentrations shown in Fig. 2 at 1000 K.

VI. SUMMARY

The electronic structure and energies of point defects in $L1_2$ Al_3Sc have been calculated using a plane-wave pseudo-

TABLE V. Expressions and numerical values for the formation energies of thermal vacancies and antisites in Al_3Sc (in eV) for small deviations from stoichiometry. The numerical values are based on the defect energies presented in Table II. Values for the stoichiomteric alloy can be taken as the average of the Al- and Sc-rich cases.

		Composition	
Defect	H_d	Al rich	Sc rich
V_{Al}	$\delta E^V(Al)+\mu_{Al}$	$E_{ref}+\delta E^V(Al)+\delta E^{Al}(Sc)/4$	$E_{ref}+\delta E^V(Al)-\delta E^{Sc}(Al)/4$
		1.792	0.884
V_{Sc}	$\delta E^V(Sc)+\mu_{Sc}$	$E_{ref}+\delta E^V(Sc)-3\,\delta E^{Al}(Sc)/4$	$E_{ref}+\delta E^V(Sc)+3\,\delta E^{Sc}(Al)/4$
		0.043	2.766
Al_{Sc}	$\delta E^{Al}(Sc)+\mu_{Sc}-\mu_{Al}$	-	$\delta E^{Sc}(Al)+\delta E^{Al}(Sc)$
		-	3.631
Sc_{Al}	$\delta E^{Sc}(Al)+\mu_{Al}-\mu_{Sc}$	$\delta E^{Sc}(Al)+\delta E^{Al}(Sc)$	-
		3.631	-

potential method. Analytical expressions for the chemical potentials and the effective formation energies were developed for an A_3B alloy near stoichiometry. The calculated defect energies were used to provide numerical estimates for these quantities in Al_3Sc at low temperatures. Calculated point defect energies were used in a dilute-solution model formalism to predict constitutional and thermal point defects as a function of alloy chemistry and temperature. The predicted constitutional defects are antisites and a small activation energy for V_{Sc} in Al-rich alloys produces a large concentration of V_{Sc}. The rate of change in defect concentration with alloy composition shown in Fig. 2 is very large, with vacancy concentrations changing by as much as ten orders of magnitude over a very narrow composition range of a fraction of a percent. The significant change in the equilbrium density of Sc vacancies with alloy composition may strongly influence the mobility of active deformation modes. Creep processes, produced by strains below the critical shear stress, are typically rate limited by diffusion. Minimizing the diffusive component of creep resistance by suppressing the population of thermal vacancies through alloy composition may be an effective design strategy for this alloy system. From the results presented here it seems likely that ternary additions may also strongly influence the concentration of thermal defects.[21] Further computational studies are currently underway to assess the effects of ternary additions on the equilibrium concentration of point defects in Al_3Sc-based alloys.

ACKNOWLEDGMENTS

This work was supported by the Air Force Office of Scientific Research and was performed at the US Air Force Research Laboratory, Materials and Manufacturing Directorate, Wright-Patterson Air Force Base under Contract No. F33615-96-C-5258. This work was supported in part by a grant of computer time from the DoD High Performance Computing Modernization Program, at the Aeronautical Systems Center-Major Shared Resource Center, on the IBM-SP2.

*Present address: Materials and Processing Division, UES Inc., 4401 Dayton-Xenia Rd., Dayton, Ohio 45432.

[1] J. H. Schneibel and E. P. George, Scr. Metall. Mater. **26**, 1823 (1990).
[2] E. P. George, J. A. Horton, W. D. Porter, and J. H. Schneibel, J. Mater. Res. **5**, 1639 (1990).
[3] J. H. Schneibel and P. M. Hazzledine, J. Mater. Res. **7**, 868 (1992).
[4] K. Fukunaga, T. Shouji, and Y. Miura, Mater. Sci. Eng., A **239-240**, 202 (1997).
[5] C. L. Fu, J. Mater. Res. **5**, 971 (1990).
[6] M. E. Dritz, L. S. Toropova, R. L. Guschina, and S. G. Fedotov, J. Sov. Non Ferrous Metal. Res. **12**, 83 (1984).
[7] R. R. Sawtell and C. L. Jensen, Metall. Trans. A **21A**, 421 (1990).
[8] M. Asta, S. M. Foiles, and A. A. Quong, Phys. Rev. B **57**, 11 265 (1998).
[9] V. Ozoliņš and M. Asta, Phys. Rev. Lett. **86**, 448 (2001).
[10] D. de Fontaine, Solid State Phys. **47**, 33 (1994).
[11] A. Zunger, in *Statics and Dynamics of Alloy Phase Transformations*, edited by P. E. A. Turchi and A. Gonis, *NATO Advanced Studies Institute, Series B: Physics*, Vol. 319 (Plenum, New York, 1994).
[12] Y. Harada and D. C. Dunand, Acta Mater. **48**, 3477 (2000).
[13] M. Hagen and M. W. Finnis, Philos. Mag. A **77**, 447 (1998).
[14] S. M. Foiles and M. S. Daw, J. Mater. Res. **2**, 1 (1987).
[15] C. L. Fu, Y. Y. Ye, M. H. Yoo, and K. M. Ho, Phys. Rev. B **48**, 6712 (1993).
[16] C. L. Fu, Phys. Rev. B **52**, 3151 (1995).
[17] J. Mayer, C. Elsä, and M. Fähnle, Phys. Status Solidi B **191**, 283 (1995).
[18] J. Mayer and M. Fähnle, Acta Mater. **45**, 2207 (1997).
[19] R. Krachler and H. Ipser, Intermetallics **7**, 141 (1999).
[20] C. Woodward, S. A. Kajihara, and L. H. Yang, Phys. Rev. B **57**, 13 459 (1998).
[21] C. Woodward and S. A. Kajihara, Acta Mater. **47**, 3793 (1999).
[22] G. G. Libowitz and J. B. Lightstone, J. Phys. Chem. Solids **28**, 1145 (1967).
[23] R. A. Johnson and J. R. Brown, J. Mater. Res. **7**, 3213 (1992).
[24] M. Hagen and M. Finnis, Mater. Sci. Forum **245**, 207 (1996).
[25] Y. Mishin and D. Farkas, Philos. Mag. A **75**, 169 (1997).
[26] Y. Mishin and D. Farkas, Scr. Mater. **39**, 625 (1998).
[27] Y. Mishin and Chr. Herzig, Acta Mater. **48**, 589 (2000).
[28] *Phase Transitions and Critical Phenomena*, edited by C. Domb and M. S. Green (Academic Press, London, 1974), Vol. 3.
[29] W. W. Mullins, in Proceedings of the International Conference on Solid-Solid Phase Transformations, edited by H. I. Aaronson, D. E. Laughlin, R. F. Sekerka, and C. M. Wayman (Met. Soc. A.I.M.E., Pittsburgh, 1982), p. 49.
[30] G. Kresse and J. Furthmueller, Comput. Mater. Sci. **6**, 5 (1996).
[31] G. Kresse and J. Furthmueller, Phys. Rev. B **54**, 11 169 (1996).
[32] G. Kresse and J. Hafner, Phys. Rev. B **47**, 558 (1993); **49**, 14 251 (1994).
[33] G. Kresse and J. Hafner, J. Phys.: Condens. Matter **6**, 8245 (1994).
[34] D. Vanderbilt, Phys. Rev. B **41**, 7892 (1990).
[35] M. Methfessel and A. T. Paxton, Phys. Rev. B **40**, 3616 (1989).
[36] F. D. Murnaghan, Proc. Natl. Acad. Sci. U.S.A. **30**, 244 (1944).
[37] H. J. Monkhorst and J. D. Pack, Phys. Rev. B **13**, 5188 (1976).
[38] J.-H. Xu and A. J. Freeman, Phys. Rev. B **41**, 12 553 (1990).
[39] R. W. Hyland, Jr. and R. C. Stiffler, Scr. Metall. **25**, 473 (1991).
[40] W. B. Pearson, *Handbook of Lattice Spacing and Structures of Metals II* (Pergammon Press, New York, 1967), Vol. 2.
[41] C. Woodward, J. M. MacLaran, and S. Rao, J. Mater. Res. **7**, 1735 (1992).